

Article ID: 1007-4627(2017)01-0051-06

# New Magicity within the Relativistic Hartree-Fock-Bogoliubov Approach

LI Jiajie, LONG Wenhui<sup>†</sup>

(School of Nuclear Science and Technology, Lanzhou University, Lanzhou 730000, China)

**Abstract:** Recent applications of the relativistic Hartree-Fock-Bogoliubov (RHFB) approach in exploring the new magicities under extreme conditions are presented for the superheavy elements with the limits of mass and charge and for the exotic nuclei with extreme neutron-to-proton ratios. It is found that the emergence of new magic shells in superheavy region is tightly related to the restoration and violation of pseudo-spin symmetry, respectively for the neutron and proton ones, in which the model deviations are indicated and discussed. In medium-heavy exotic nuclei, the occurrence of new magicity  $N = 32, 34$  in Ca isotopes is well reproduced by the RHFB approach, in which the isovector Lorentz tensor couplings are found to play an essential role. The results exemplify that the RHFB approach, which considers the exchange (Fock) terms explicitly, furnishes a new theoretical instrument for advancing relativistic nuclear mean-field approaches.

**Key words:** new magicity; exotic nuclei; superheavy nuclei; pseudo-spin symmetry; tensor force

**CLC number:** O571.6      **Document code:** A      **DOI:** 10.11804/NuclPhysRev.34.01.051

## 1 Introduction

The atomic nuclei are self-bound many-body systems which have to be treated with the many-body quantum theory. They exhibit a rich variety of phenomena due to spin, isospin and eventually strangeness degrees of freedom of the strong interaction. In addition, the correlations induced by various symmetry breaking such as deformation and pairing for instance, make atomic nucleus be a very interesting and complex system. The exploration of nuclei far from stability represents a new frontier in our understanding of nuclear structure and nuclear astrophysics.

In this contribution, we report on our recent investigations of the possible occurrence of new magic number located at the limit of stability for very large masses (superheavy nuclei) and extreme isospin asymmetric systems (exotic nuclei). The motivations for this endeavour are based on the new possibilities offered by the relativistic Hartree-Fock-Bogoliubov (RHFB) theory<sup>[1]</sup> which has made a major step forward in the recent years.

The advantages of a covariant mean-field approach for such a study are well established. In the

nonrelativistic mean-field method<sup>[2]</sup>, the central and spin-orbit (SO) potentials depend on different parts of the energy density functional and therefore, on independently adjusted parameters of the functional. In the relativistic energy density functional, on the other hand, all parameters of the functional contribute to the Lorentz scalar and vector mean fields, etc., and to the SO potential of the nucleonic Dirac equation are not independent. In contrast to the relativistic mean-field (RMF) approach<sup>[3, 4]</sup> in which the Fock diagrams are simply dropped, the relativistic Hartree-Fock (RHF) approach provides a relativistic platform to account for the nuclear tensor force naturally<sup>[5-7]</sup>. These aspects are quite crucial obviously when one tries to predict magic structures in unknown regions of the nuclear landscape.

## 2 Relativistic Hartree-Fock-Bogoliubov approach

We briefly sketch the theoretical framework used here to describe the ground-state properties of nuclei. The model consists of a Lagrangian  $\mathcal{L}$  containing two parts. The first part  $\mathcal{L}_{\text{free}}$  is a sum of terms describ-

**Received date:** 18 Sep. 2016;    **Revised date:** 3 Oct. 2016.

**Foundation item:** National Natural Science Foundation of China(11375076, 11675065); Specialized Research Fund for Doctoral Program of Higher Education (20130211110005)

**Biography:** LI Jiajie(1986-), male, Lanzhou, Gansu, Ph.D, working on nuclear physics

<sup>†</sup> **Corresponding author:** LONG Wenhui, E-mail: longwh@lzu.edu.cn.

ing the free nucleon field, free meson and photon fields. The second part  $\mathcal{L}_1$  represents the nucleon-nucleon interaction mediated by the meson and photon fields. This interaction Lagrangian can be expressed as:

$$\mathcal{L}_1 = \bar{\psi} \left( -g_\sigma \sigma - g_\omega \gamma^\mu \omega_\mu - g_\rho \gamma^\mu \boldsymbol{\rho}_\mu \cdot \boldsymbol{\tau} + \frac{f_\rho}{2M} \sigma_{\mu\nu} \partial^\nu \boldsymbol{\rho}^\mu \cdot \boldsymbol{\tau} - \frac{f_\pi}{m_\pi} \gamma_5 \gamma_\mu \partial^\mu \boldsymbol{\pi} \cdot \boldsymbol{\tau} - e \gamma^\mu A_\mu \frac{1-\tau_3}{2} \right) \psi, \quad (1)$$

which contains the  $\sigma$ -scalar ( $\sigma$ -S),  $\omega$ -vector ( $\omega$ -V),  $\rho$ -vector ( $\rho$ -V),  $\rho$ -tensor ( $\rho$ -T),  $\pi$ -pseudo-vector ( $\pi$ -PV) and photon-vector ( $A$ -V) couplings, and the meson-nucleon couplings  $g_i$  and  $f_i$  are density-dependent<sup>[8, 9]</sup>. Applying the standard variations of the Lagrangian, one may obtain the field equations for nucleon, meson, and photon fields, as well as the RHF Hamiltonian.

Incorporating the standard Bogoliubov transformation, it leads to the RHF approach which provides a unified and self-consistent description of both particle-hole (ph) and particle-particle (pp) channels at the mean-field level. The RHF equation in coordinate representation reads as,

$$\int d\mathbf{r}' \begin{pmatrix} h(\mathbf{r}, \mathbf{r}') & \Delta(\mathbf{r}, \mathbf{r}') \\ -\Delta(\mathbf{r}, \mathbf{r}') & h(\mathbf{r}, \mathbf{r}') \end{pmatrix} \begin{pmatrix} \psi_U(\mathbf{r}') \\ \psi_V(\mathbf{r}') \end{pmatrix} = \begin{pmatrix} \lambda + E & 0 \\ 0 & \lambda - E \end{pmatrix} \begin{pmatrix} \psi_U(\mathbf{r}) \\ \psi_V(\mathbf{r}) \end{pmatrix}, \quad (2)$$

where  $E$  is the quasiparticle energy,  $\psi_U$  and  $\psi_V$  are the spinors of Bogoliubov quasiparticle, and the chemical potential  $\lambda$  is introduced to preserve the particle number on the average. The Dirac single-particle (s.p.) Hamiltonian  $h$ , which encloses the  $ph$  correlations with mean field approach, is of the form

$$h(\mathbf{r}, \mathbf{r}') = (\boldsymbol{\alpha} \cdot \mathbf{p} + \beta M) + \Sigma_H(\mathbf{r}) \delta(\mathbf{r} - \mathbf{r}') - \Sigma_F(\mathbf{r}, \mathbf{r}'). \quad (3)$$

Here the local field  $\Sigma_H$  contains the contributions from the Hartree and the rearrangement terms, and the non-local one  $\Sigma_F$  corresponds to the Fock terms<sup>[8, 9]</sup>.

The pairing field  $\Delta$ , which represents the pp correlations, reads as:

$$\Delta_\alpha(\mathbf{r}, \mathbf{r}') = -\frac{1}{2} \sum_\beta V_{\alpha\beta}^{\text{PP}}(\mathbf{r}, \mathbf{r}') \kappa_\beta(\mathbf{r}, \mathbf{r}'), \quad (4)$$

with  $\kappa$  being pairing tensor. In practice, the phenomenological finite-range Gogny force<sup>[10]</sup> are used in the pairing channels, namely  $V^{\text{PP}}$ , to obtain reasonable pairing effects.

With the help of the relativistic formalism of nuclear tensor force<sup>[6]</sup>, the one- $\pi$  exchange potential  $V_\pi$

can be divided into two terms: the tensor and the central potentials,  $V_\pi^{\text{T}}$  and  $V_\pi^{\text{C}}$ . The tensor force component in  $\pi$ -PV coupling reads as,

$$H_\pi^{\text{T}} = -\frac{1}{2} \left[ \frac{f_\pi}{m_\pi} \bar{\psi}_\alpha \gamma_0 \Sigma_\mu \boldsymbol{\tau} \psi_\beta \right]_1 \cdot \left[ \frac{f_\pi}{m_\pi} \bar{\psi}_\beta \gamma_0 \Sigma_\nu \boldsymbol{\tau} \psi_\alpha \right]_2 D_\pi^{\text{T}, \mu\nu}(1, 2), \quad (5)$$

$$D_\pi^{\text{T}, \mu\nu} = \left[ \partial^\mu(1) \partial^\nu(2) - \frac{1}{3} g^{\mu\nu} m_\pi^2 \right] \times \frac{e^{-m_\pi |\mathbf{x}_1 - \mathbf{x}_2|}}{|\mathbf{x}_1 - \mathbf{x}_2|} + \frac{1}{3} g^{\mu\nu} \delta(x_1 - x_2). \quad (6)$$

Relevant tensor force components in  $\rho$ -T couplings can also be extracted with the formalism in Ref. [7]. One must notice that, in the nonrelativistic formalism, the central and rank-2 tensor forces generally appear independently from each other, while here they originate from the same interaction vertices.

Concerning numerical calculations, the coupled integro-differential Eq. (2) are solved in a Dirac Woods-Saxon basis<sup>[11]</sup>. Such a model is appropriate for describing stable as well as loosely bound nuclei since the basis states have the correct asymptotic behavior for large spatial distributions.

### 3 Prediction of new magic numbers

#### 3.1 Superheavy magic structures

In ordinary nuclei, the magicity is generally well marked, *e.g.*, by a sizable shell gap along the isotopic or isotonic chains. In Superheavy nuclei (SHN), the shell effects are not so clearly visible. To identify the magic shells it is convenient to look at the two-nucleon gaps —  $\delta_{2p}$  for protons and  $\delta_{2n}$  for neutrons, namely the differences of two-nucleon separation energies of the neighboring isotopes or isotones.

We have explored the evolution of  $\delta_{2p}$  and  $\delta_{2n}$  for the nuclei covering the ranges  $110 \leq Z \leq 140$  and  $140 \leq N \leq 280$ , using the 6 Lagrangians — the RHF ones PKO1, PKO2, PKO3 and PKA1, and the RMF ones PKDD and DD-ME2. The calculated values of  $\delta_{2p}$  and  $\delta_{2n}$  vary from 1 to 5 MeV. As a general result, PKA1 is the model which predicts the larger two-nucleon gaps (3 to 5 MeV) for  $Z = 120, 126, 138$  and  $N = 184, 258$ . Therefore, these are the candidates of superheavy magicity well supported by PKA1. The other Lagrangians also indicate a well marked proton closed shell at  $Z = 120$  and 138.

Concerning the neutron shells, the predictions vary with the particular model Lagrangian employed. At  $N = 172$  and 228, neutron shell closures are found with the various Lagrangians considered here, although the shell effects appear to be rather weak.

Other predicted neutron magic numbers are  $N = 184$  and 258 (except with PKO2). By examining the predictions of the various models discussed here, one may tentatively conclude that the nuclide  $^{304}120_{184}$  could be a doubly magic system, and  $^{292}120_{172}$  might be another, less stable candidate.

Such distinct deviations, in general, can be interpreted in term of the bulk properties of symmetric nuclear matter determined by the present sets of Lagrangians, *i.e.*, the scalar (Dirac) mass  $M_S^*$  and effective mass  $M_{NR}^*$ , which essentially determine the strength of SO couplings and level densities, respectively. This aspect is largely detailed in Ref. [12].

It is interesting to examine the significance of the magic numbers  $Z = 120$ ,  $N = 184$  in the light of the pseudospin symmetry (PSS)<sup>[13]</sup> and its breaking. In realistic nuclei, the PSS is in general conserved approximately due to the delicate balance between strong attraction and repulsion represented by the scalar poten-

tial and the vector one, respectively. Thus, the amount of PSS violation will affect the relative positions of the partners, and therefore the  $N$  and  $Z$  numbers corresponding to filled subshells.

This is illustrated in Fig. 1 by the single-particle (s.p.) spectra of the nuclide  $^{304}120_{184}$  calculated with various Lagrangians. One can see that the PSS is sometimes fairly well obeyed, *e.g.*, for the doublet ( $\nu 4s_{1/2}$ ,  $\nu 3d_{3/2}$ ) and sometimes strongly broken, *e.g.*, for the doublets ( $\nu 2h_{11/2}$ ,  $\nu 1j_{13/2}$ ) and ( $\pi 3p_{3/2}$ ,  $\pi 2f_{5/2}$ ). In the case of the proton states, the magic number  $Z = 120$  just corresponds to the lower partner  $\pi 2f_{5/2}$  completely filled and the upper partner  $\pi 3p_{3/2}$  empty. Indeed, for all the models shown in Fig. 1 there is a large splitting - of the order of 2 MeV - for the pseudospin partners ( $\pi 2f_{5/2}$ ,  $\pi 3p_{3/2}$ ), while the SO splitting of the  $\pi 3p$  levels is fairly small. This is mainly due to the appearance of semibubble formation at  $Z = 120$  superheavy systems<sup>[14]</sup>.

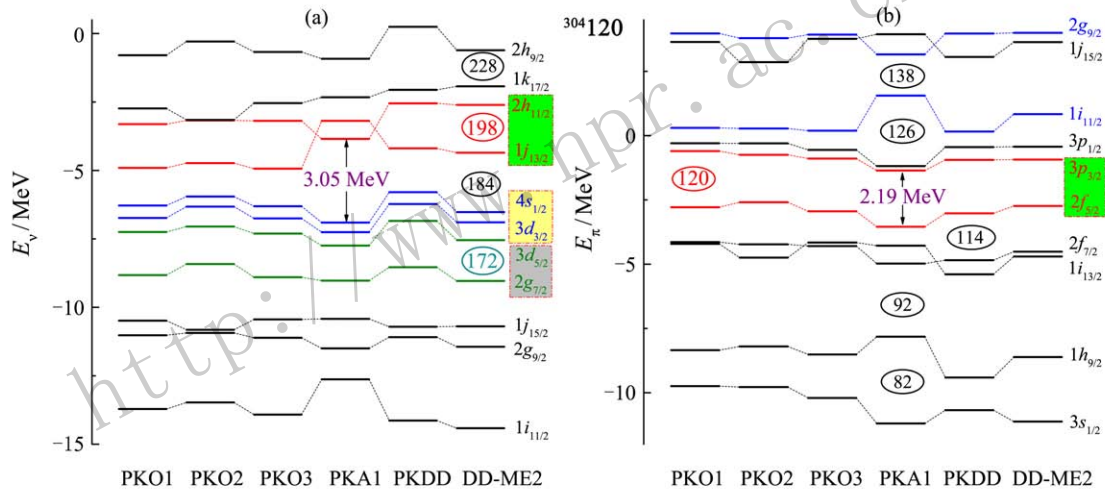


Fig. 1 (color online) Neutron (a) and proton (b) single-particle spectra in the  $^{304}120$  nuclide. The results with PKO1 and PKA1 correspond to RHF calculations, those with PKDD and DD-ME2 are obtained in RHB approximation.

On the neutron side, we observe that the prediction of PKA1 for the pseudospin partners ( $\nu 1j_{13/2}$ ,  $\nu 2h_{11/2}$ ) is very different from that of the 5 other models, with a smaller splitting and a reversed order. We recall that the PKA1 Lagrangian contains an extra degree of freedom as compared to the other models, namely a Lorentz tensor  $\rho$ -N coupling. This is probably the reason for the different ( $\nu 1j_{13/2}$  -  $\nu 2h_{11/2}$ ) splitting.

### 3.2 Magicity of neutron-rich Ca isotopes

Since the tensor interaction that contributes in Ca isotopes above  $^{40}\text{Ca}$  is mostly active between a few neutron states: mostly  $\nu 2p$  and  $\nu 1f$  states, Ca isotopes therefore provide an ideal isotopic chain for the

theoretical and experimental analysis of the tensor interaction and for studying its role in the formation and evolution of neutron shells in medium mass nuclei.

By analyzing the question of possible proton level inversion in  $^{48}\text{Ca}$ , we found that the Lorentz tensor  $\rho$ -field is an important ingredient for the restoration of PSS, namely the proton  $sd$  degeneration, in  $^{48}\text{Ca}$ <sup>[14]</sup>. The importance of the tensor force in this context has also been stressed by nonrelativistic approaches<sup>[16]</sup>. It provides therefore a good motivation to investigate more neutron-rich Ca isotopes with RHF functionals.

From the experimental side, the high excitation energy of  $^{52}\text{Ca}$ , compared to those of neighbouring nuclei, favors a possible new  $N = 32$  shell closure<sup>[17]</sup>. Then, a confirmation was obtained from recent high-

precision mass measurements of several isotopes ranging from  $^{51}\text{Ca}$  up to  $^{54}\text{Ca}$  [18]. Additionally, from the very recent measurement of the  $2_1^+$  energy in  $^{54}\text{Ca}$  which was found to be only  $\sim 500$  keV below that in  $^{52}\text{Ca}$  [19], it is also possible that  $^{54}\text{Ca}$  could be magic as well.

Fig. 2 shows the isotopic evolution of the s.p. energies (upper panels) and average pairing gaps (lower panels) from  $^{40}\text{Ca}$  to  $^{60}\text{Ca}$ , going over the possible new magic numbers at  $N = 32$  and  $34$ , and using RH(F)B approach with the selected effective Lagrangians: PKA1 and DD-ME2. The general feature

is that, as the number of neutrons increases, the s.p. energies decrease due to the enhanced mean-field potential. This trend is smooth for the DD-ME2, while we observe abrupt changes in the PKA1 results when the s.p. energies cross the Fermi energy. Notice moreover that  $^{40}\text{Ca}$  is spin-saturated, while the spin asymmetry reaches the maximal at  $^{52}\text{Ca}$ . We have analysed the isotopic evolution of the two-body interaction matrix elements  $V_{ii'}$  between neutron valence orbits and we found that the couplings are quite constant for the DD-ME2 while for the PKA1 they are slightly more dependent on the number of neutrons.

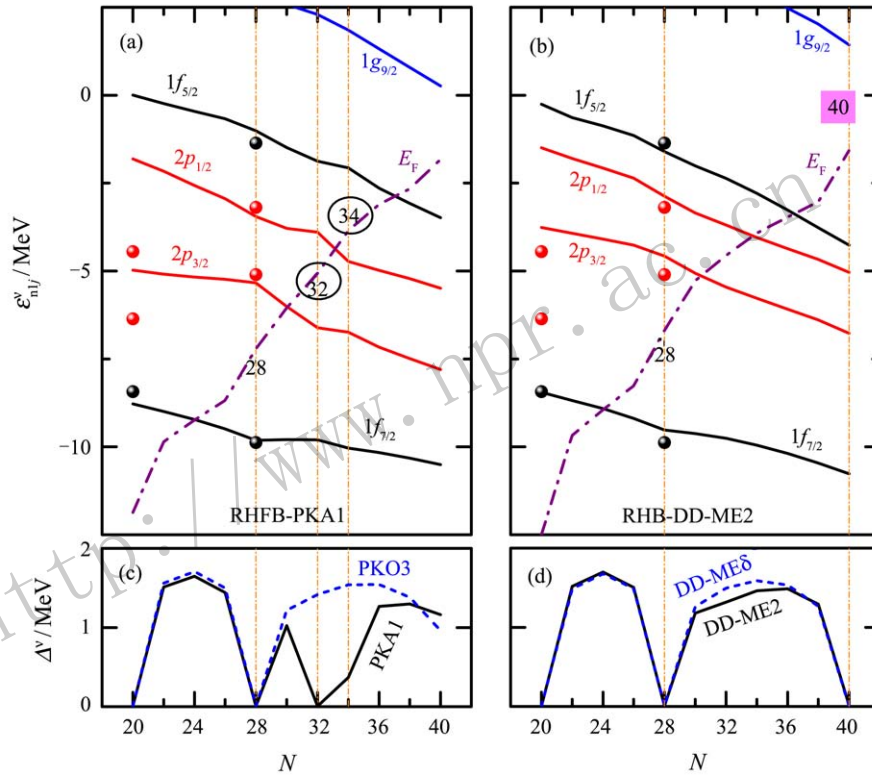


Fig. 2 (color online) Neutron s.p. spectra and pairing gaps of Ca isotopes, extracted from RHF(B) with PKA1 (a) and RHF(B) with DD-ME2 (b). The experimental data (in spheres) are taken from Ref. [15].

The magicity is not solely related to an increase of the shell gap, but also to a quenching of the pairing correlations. As seen from Figs. 2(c) and (d), the suppression of the neutron pairing gaps at traditional magic numbers  $N = 20$  and  $28$  is confirmed by all the models considered here. In the PKA1 results, there is an additional suppression of the neutron pairing gap at  $N = 32$  which is not predicted by the other Lagrangians. This large quenching for  $N = 32$  is an additional hint which suggests that the  $N = 32$  magic number should be analyzed in the light of the Lorentz PV and T interactions. A weaker, but still distinct and important, quenching

is also predicted by the PKA1 at  $N = 34$ , which may suggest as well  $N = 34$  to be a submagic number.

We now analyze the evolution of  $N = 32, 34$  shell gaps and the role of the Lorentz PV and T interactions. Fig. 3(a) shows the contribution of the Lorentz PV and T couplings to the  $\nu 2p$  splittings along  $N = 32$  isotonic chain. In order to better analyze the isotonic evolution, we present the results with respect to the value calculated in Ca. Here, we truncate at S to make the figures more readable, but the conclusions extend beyond. We find that the Lorentz PV and T couplings play a dominant role in determining the enhancement of the  $2p$

SO splitting from Ni to Ca, while from Ca to S, the contributions of the Lorentz PV and T couplings are close to zero. In addition, it is worth noticing the large contribution of the central term to the SO splitting between Ni and Ca, while the rank-2 tensor accounts for

only 30% of the increase. It is thus illustrated in the case of the  $N = 32$  isotones that the effects of the Lorentz PV and T on the s.p. energy gaps is certainly not reducible to the contribution of the rank-2 tensor because the central term plays a more important role.

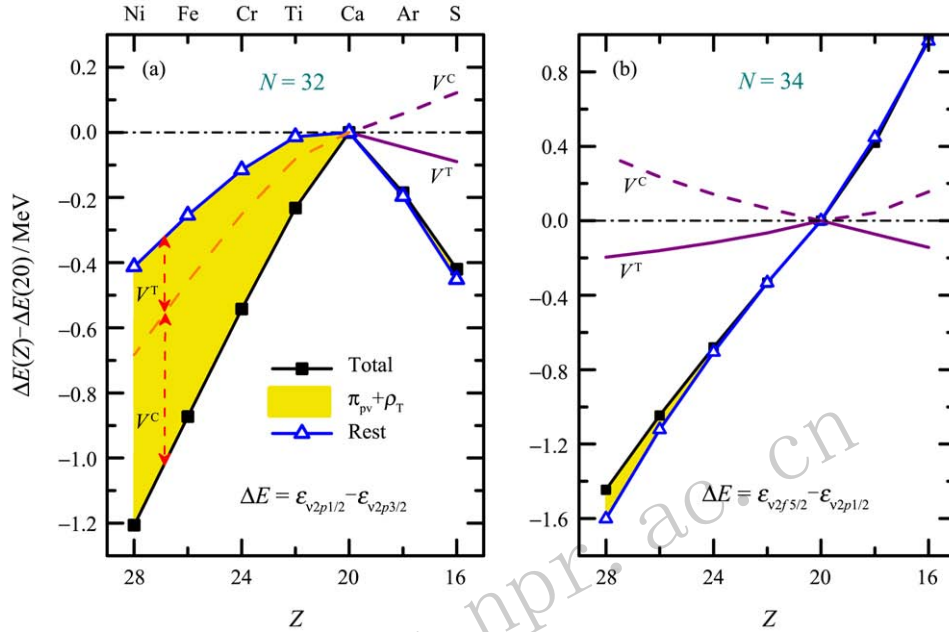


Fig. 3 (color online) Detailed contributions to the energy difference  $\Delta E(i, i') \equiv \varepsilon_i - \varepsilon_{i'}$  in  $N = 32$  (a) and  $34$  (b) isotones from the Lorentz PV and T components ( $\pi$ -PV +  $\rho$ -T), in comparison with those from the other components. The results are extracted from RHFb with PKA1.

The situation for  $N = 34$  gap which appears between the  $\nu 2p_{1/2}$  and  $\nu 1f_{5/2}$  states is different. In this case the role of the Lorentz PV and T is not so straightforward since both are the  $j_<$  states. It is found, for PKA1, that the Lorentz PV and T forces present tiny contributions to the splitting between the  $\nu 2p_{1/2}$  and  $\nu 1f_{5/2}$  states. As shown in Fig. 3(b) the origin of this weakening is due to the near cancellation between the central and the rank-2 tensor components of the Lorentz PV and T forces. However, the shell gaps continue to increase between  $^{52}\text{Ar}$  and  $^{50}\text{S}$ , and this tendency is confirmed for the next  $N = 34$  nucleus  $^{48}\text{Si}$ . PKA1 predicts a large gap for the drip line nucleus  $^{48}\text{Si}$  ( $\sim 4.0$  MeV) and a small pairing gap.

## 4 Conclusion

The RHFb approach has been applied to the self-consistent predictions of new magicity under extreme conditions. Particular focus is placed on roles of the Fock terms. The effect of Fock terms is significant to describe nuclear shell structure reasonably well. Several examples have been presented: (i) proton  $sd$  degeneration (inversion) in Ca isotopes, to which the Lorentz tensor force gives correct  $N$ -dependence, (ii)

prediction of magic numbers in neutron-rich Ca isotopes, to which the PKA1 Lagrangian gives results compatible with available experimental information, (iii) superheavy magic structures, to which the shell effects are sensitive to various terms of the mean-field, such as the SO coupling, the scalar and effective masses. It is now clear that the modelling of exotic nuclei requires the development of more complete nuclear effective interactions. For instance, at a relativistic framework the exchange (Fock) terms should be explicitly treated rather than approximately included by reorganized direct (Hartree) contributions.

## References:

- [1] LONG W H, RING P, VAN GIAI N, *et al.* Phys Rev C, 2010, **81**: 024308.
- [2] BENDER M, HEENEN P H, REINHARD P G. Rev Mod Phys, 2003, **75**: 121.
- [3] VRETENAR D, AFANASJEV A V, LALAZISSIS G A, *et al.* Phys Rep, 2005, **409**: 101.
- [4] MENG J, TOKI H, ZHOU S G, *et al.* Prog Part Nucl Phys, 2006, **57**: 470.
- [5] LONG W, SAGAWA H, MENG J, *et al.* Europhys Lett, 2008, **82**: 12001.

- [6] JIANG L J, YANG S, SUN B Y, *et al.* Phys Rev C, 2015, **91**: 034326.
- [7] LI J J, MARGUERON J, LONG W H, *et al.* Phys Lett B, 2016, **753**: 97.
- [8] LONG W H, SAGAWA H, VAN GIAI N, *et al.* Phys Rev C, 2007, **76**: 034314.
- [9] LONG W H, VAN GIAI N, MENG J. Phys Lett B, 2006, **640**: 150.
- [10] BERGER J F, GIROD M, GOGNY D. Nucl Phys A, 1984, **428**: 23.
- [11] ZHOU S G, MENG J, RING P. Phys Rev C, 2003, **68**: 034323.
- [12] LI J J, LONG W H, MARGUERON J, *et al.* Phys Lett B, 2014, **732**: 169.
- [13] LIANG H, MENG J, ZHOU S G. Phys Rep, 2015, **570**: 1.
- [14] LI J J, LONG W H, SONG J L, *et al.* Phys Rev C, 2016, **93**: 054312.
- [15] GRAWE H, LANGANKE K, MARTÍNEZ-PINEDO G. Rep Prog Phys, 2007, **70**: 1525.
- [16] NAKADA H, SUGIURA K, MARGUERON J. Phys Rev C, 2013, **87**: 067305.
- [17] GADE A, JANSSENS R V F, BAZINPHYS D, *et al.* Rev C, 2006, **74**: 021302.
- [18] WIENHOLTZ F, BECK D, BLAUM K, *et al.* Nature, 2013, **498**: 346.
- [19] STEPPENBECK D, TAKEUCHI S, AOI N, *et al.* Nature, 2013, **502**: 207.

## 基于相对论 Hartree-Fock-Bogoliubov 近似的新幻数研究

李佳杰, 龙文辉<sup>†</sup>

(兰州大学核科学与技术学院, 兰州 730000)

**摘要:** 基于相对论 Hartree-Fock-Bogoliubov (RHFB) 近似分别探索了质量-电荷极限下的超重元素与极端中质比下的奇特原子核中的新幻数问题。研究表明, 赝自旋对称性的守恒和破缺与超重核区球形幻数结构的形成密切相关, 并分别决定了中子与质子的新幻数结构。同时, 理论模型之间的差异也与之密切相关。在中重奇特核区, RHFB 近似很好地再现了 Ca 同位素中的新幻数  $N = 32, 34$ , 其中同位旋矢量道中洛伦兹张量耦合扮演了较为关键的角色。以此为例, 研究证明了显式考虑交换 (Fock) 项的 RHFB 近似的可靠性。

**关键词:** 新幻数; 奇特核; 超重核; 赝自旋对称性; 张量力

收稿日期: 2016-09-18; 修改日期: 2016-10-03

基金项目: 国家自然科学基金资助项目(11375076, 11675065); 教育部博士点基金博导类项目(20130211110005)

<sup>†</sup> 通信作者: 龙文辉, E-mail: longwh@lzu.edu.cn.